Automatic multimodal 2D/3D image fusion of Ultrasound Computer Tomography and X-ray mammography for breast cancer diagnosis

Torsten Hopp[a], Neb Duric[b], Nicole V. Ruiter[a]

[a]Karlsruhe Institute of Technology, Institute for Data Processing and Electronics, Karlsruhe, Germany;
[b]Barbara Ann Karmanos Cancer Institute, Department of Radiation Oncology, Detroit, USA

ABSTRACT

Breast cancer is the most common cancer among women. The established screening method to detect breast cancer in an early state is X-ray mammography. However, X-ray frequently provides limited contrast of tumors located within glandular tissue. A new imaging approach is Ultrasound Computer Tomography generating three-dimensional volumes of the breast. Three different images are available: reflectivity, attenuation and speed of sound. The correlation of USCT volumes with X-ray mammograms is of interest for evaluation of the new imaging modality as well as for a multimodal diagnosis. Yet, both modalities differ in image dimensionality, patient positioning and deformation state of the breast. In earlier work we proposed a methodology based on Finite Element Method to register speed of sound images with the according mammogram. In this work, we enhanced the methodology to register all three image types provided by USCT. Furthermore, the methodology is now completely automated using image similarity measures to estimate rotations in datasets. A fusion methodology is proposed which combines the information of the three USCT image types with the X-ray mammogram via semi-transparent overlay images. The evaluation was done using 13 datasets from a clinical study. The registration accuracy was measured by the displacement of the center of a lesion marked in both modalities. Using the automated rotation estimation, a mean displacement of 10.4 mm was achieved. Due to the clinically relevant registration accuracy, the methodology provides a basis for evaluation of the new imaging device USCT as well as for multimodal diagnosis.

Keywords: Registration, Ultrasound Computer Tomography, Mammography, Image fusion, Multimodal diagnosis

1. INTRODUCTION

Throughout Northern America and Europe, breast cancer is the most common cancer among women.[1] Approximately 230,400 new cases of invasive breast cancer and additional 57,600 cases of in situ breast cancer are expected to be diagnosed in the US in 2011. 39,500 women are expected to die from breast cancer every year. Only lung cancer causes more cancer deaths in women.[2] Detection of breast cancer in an early state is essential for an effective treatment since the likelihood of developing metastases is correlated to the size of the tumor.[3] Today medical imaging provides the method of choice for early breast cancer detection.

Currently X-ray mammography is the established screening method. It provides high resolution images and is capable of visualizing e.g. microcalcifications. However X-ray frequently provides poor contrast for tumors located within glandular tissue and only displays a projection of a deformed breast. In clinical routine, Magnetic Resonance Imaging (MRI) is used additionally for definite diagnosis, offering high contrast of soft tissue and high diagnostic accuracy.[4] Yet during MRI acquisition, usually contrast agent has to be administered to the patient to visualize lesion vasculature. In consequence MRI is far more expensive and not as widespread as X-ray mammography.[5]

torsten.hopp@kit.edu, phone +49 721 608 2 5990, adress: Hermann-von-Helmholtz-Platz 1, Eggenstein-Leopoldshafen 76344, Germany, http://www.ipe.kit.edu/

Medical Imaging 2012: Ultrasonic Imaging, Tomography, and Therapy, edited by Johan G. Bosch, Marvin M. Doyley, Proc. of SPIE Vol. 8320, 83200P · © 2012 SPIE
CCC code: 1605-7422/12/$18 · doi: 10.1117/12.911156

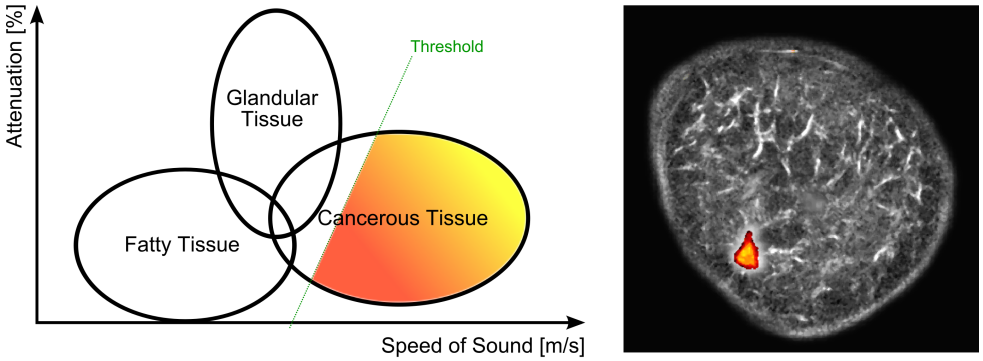

Figure 1: Relation between the ultrasonic properties speed of sound and attenuation for different breast tissues (adapted and simplified from *Greenleaf et al.*[9]). A threshold on attenuation and speed of sound is used to highlight suspect tissue within the USCT volume.

A new approach for breast imaging is Ultrasound Computer Tomography (USCT), which offers three-dimensional volumes of the breast in prone position.[6–8] The imaging is based on numerous ultrasound transducers, which surround the breast within a water bath. USCT provides three types of images: reflection images, attenuation images and speed of sound images. Reflection images reveal changes in the echotexture and are therefore able to image the surface of tissues. This results in the visualization of the morphology. Attenuation and speed of sound images are expected to provide tissue characterization. A high speed of sound and a high attenuation compared to surrounding fatty tissue respectively a high speed of sound and a low attenuation compared to surrounding glandular tissue is expected to be an indicator of cancerous tissue (Figure 1 left).[9] All three modalities are usually fused to display the breast architecture, parenchyma and suspicious lesions simultaneously (Figure 1 right).[7]

The correlation of USCT volumes and X-ray mammograms is challenging due to the different dimensionality of images, different patient positioning and different deformation states of the breast. Since USCT is still in development, comparison of images with the standard screening method mammography is of interest for quality measurement, e.g. the correlation of histologically verified findings in the mammogram with the corresponding region in the USCT volume. Furthermore the fusion of diagnostic information may benefit combined reading in radiological diagnosis. Especially for dense breast tissue, characterization by attenuation and speed of sound images may provide a guidance for diagnosis of cancerous lesions.

In earlier work we presented a method for the registration of X-ray mammograms and speed of sound volumes[10] based on an algorithm originally designed for the registration of X-ray mammograms and MRI volumes.[11] It is based on a patient-specific biomechanical model to simulate the huge deformation which is applied to the breast during mammography. The model is described as Finite Element Model (FEM) and built based on the speed of sound volumes. The FEM simulation than mimicks the mammographic compression resulting in a similar configuration of the speed of sound volume as in a corresponding mammogram. The projection of the deformed speed of sound volume showed overlaying circumferences with the mammogram. Hence, both modalities could be compared directly and overlay images providing visualization of speed of sound on mammograms could be created for intuitive diagnosis.[12] Yet the application of this method to all three image types provided by USCT was not carried out before. Furthermore accuracy of the methodology was dependent on manual corrections of the preprocessing.

In this paper we present a fully automated methodology and first image fusion results of all three image types provided by USCT and X-ray mammograms. Section 2 explains the registration approach followed the evaluation with 13 clinical datasets in section 3. Finally, section 4 concludes the paper and presents an outlook on current and future work.

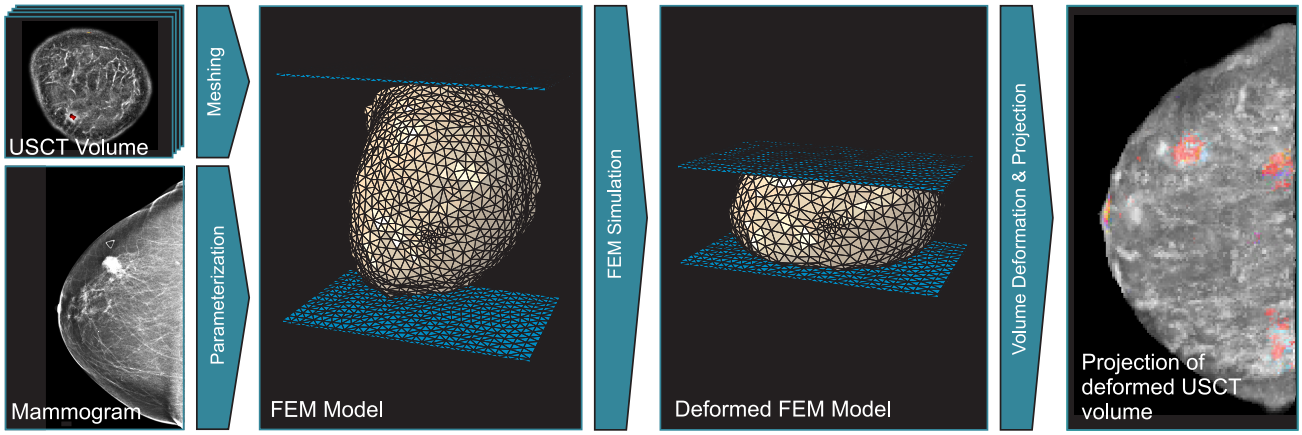

Figure 2: Simplified principle of the registration process. A FEM model is created on basis of the preprocessed USCT volume using a meshing algorithm. The model is parameterized by information from the mammogram. Afterwards the compression simulation is carried out. Based on the deformed FEM model, the USCT volume is deformed and projected creating an image directly comparable to the mammogram.

2. METHODS

The challenge of the image registration is that X-ray mammograms are two-dimensional projections of the breast in a deformed configuration whereas USCT volumes present the three-dimensional undeformed breast. This conflict is solved using a biomechanical model to estimate the relation between deformed and undeformed breast. The deformation is determined by a compression simulation based on the Finite Element Method (FEM). The underlying patient specific biomechanical model is built on the basis of the preprocessed USCT volume (Figure 2).

2.1 Composition of USCT Volumes

USCT volumes are acquired at Karmanos Cancer Institute (KCI) using a clinical prototype and a standardized acquisition procedure. Reflection images I_R are fused with the thresholded attenuation images I_A and the thresholded speed of sound images I_S for improved visualization according to the following formula:[7]

$$I_F = \left[I_R + I_{S=a}^{S=b}\right] + \left[I_{S>c} \bullet I_{A>d}\right]$$

where $\bullet$ denotes the logical AND-operation and a, b, c, d are variable thresholds. The final image displays the breast architecture and the parenchyma as grayscale image (first term of right hand side). Suspicious lesions are shown as colored region (last term of right hand side, e.g. Figure 1).

To carry out the image fusion of a mammogram with the corresponding USCT volume, several processing steps have to be performed (Figure 3). In the following subsections, each step is presented.

2.2 Image Preprocessing

Fused USCT volume I_F as well as the corresponding mammogram have to be preprocessed. The mammogram is scaled to meet the resolution of the USCT volume. Rotations are performed to match the internally used coordinate system. An interpolation in anterior direction is applied to the USCT volume to obtain isotropic voxels. Afterwards images are segmented into background and object using a provided presegmentation by KCI, thresholding and morphological operations.

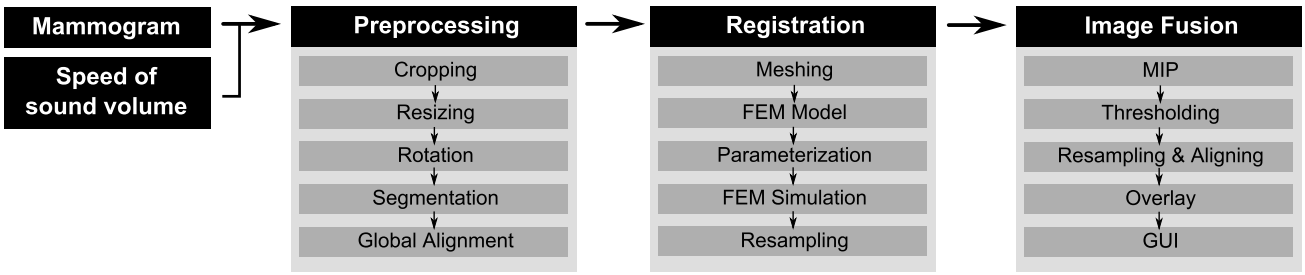

Figure 3: Workflow of the fusion process: first images have to be preprocessed, afterwards the model-based registration is carried out. Finally the visualization process creates the fused images of X-ray mammograms and USCT volumes.

2.3 Registration

On basis of the preprocessed USCT volume, a patient-specific biomechanical model is built up. To describe the geometry of the model a tetrahedral meshing is applied.[13] The physical behavior of the model is described by a material model and boundary conditions. We assume the breast tissue to be an incompressible material resulting in only a shape change, not in a change of volume. The incompressibility is approximated by a Poisson's ratio near 0.5. The stress-strain relationship of the breast tissue is described by a neo-hookean material model and using homogeneous tissue. We use material parameters as proposed by *Wellman et al.*[14] Nodes at the back of the model are fixed in anterior direction to model the fixation of the breast at the chest wall.

Boundary conditions are formulated via parameterization of the model by information obtained from the mammogram. The mammographic compression is mimicked by a two step approach. In the first step, compression plates modeled of a acrylic glass like material are added to the simulation. The deformation is carried out by moving the compression plates until a defined amount of compression is achieved. The interface between breast and plates is modeled without friction. Due to simplifications and uncertainties in this process, images do not overlap congruently after carrying out the first simulation step. Hence the second step compensates the deviation between deformed USCT volume (outcome of the first compression step) and the mammogram. A target model is built up based on the segmented mammogram and displacement vectors between deformed USCT volume and target model are defined on a closest point basis. The displacement vectors are applied as new boundary conditions for a second FEM simulation resulting in a configuration of the USCT volume showing congruently overlapping circumferences with the mammogram. Due to this, a projection image of the deformed USCT volume can be spatially compared directly to the mammogram. For more details on the registration process refer to Hopp et al.[10,15]

2.4 Intensity-Based Rotation Optimization

Uncertainties in patient positioning and rotation angle of the images might cause less accurate results than proposed by the original method.[11] We approximate this misregistration by rotating the USCT volume around the sagittal axis before starting the registration process described in section 2.3. While the rotation angle was estimated manually in earlier work,[12] the software is now enhanced using an intensity-based optimization. The projection of the deformed USCT volume after the second simulation step and the corresponding mammogram are compared using a image similarity measure $\mathbf{S}$. The registration $\mathbf{R}$ using rotation angle α delivering the best value for $\mathbf{S}$ is used as final result:

$$\arg\max\left(\mathbf{S}\left(\mathbf{R}\left(\alpha\right)\right)\right)$$

Due to the use of all three image types provided by USCT, architectural information is available, which we expect to correlate with the internal structures of the breast visible in the mammogram. Different image similarity measures were compared: normalized mutual information with different binning, correlation coefficient, partitioned intensity uniformity, ratio-image uniformity,[16] gradient difference and gradient correlation.[17]

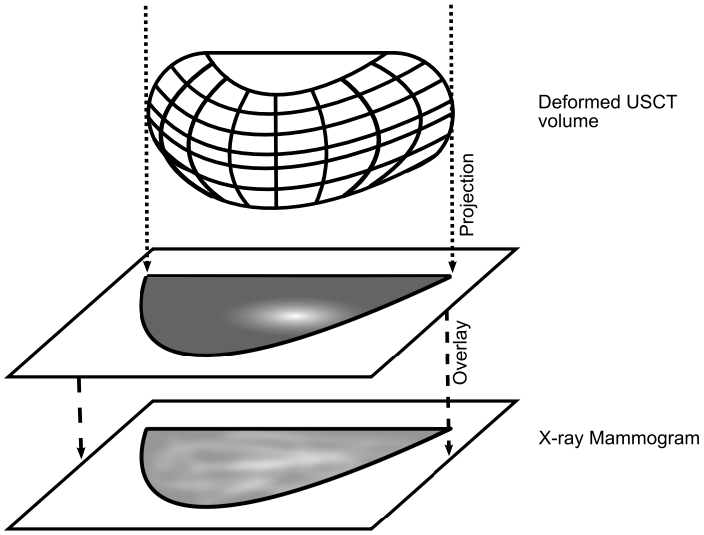

Figure 4: Generation of overlay on mammograms: a projection of the deformed USCT volume is used to superimpose the original mammogram.

2.5 Image Fusion

In order to combine the three image types provided by USCT with the corresponding mammogram in a single image, the maximum intensity projection of the deformed USCT volume I_F is used to create a semi-transparent overlay image on the mammogram (Figure 4). Regions showing a speed of sound greater c and an attenuation greater d are extracted, color-coded and rendered on the mammogram while all other pixels of the overlay image are set transparent.

3. RESULTS

For evaluation of the registration, 13 datasets from a clinical study[7] of the Karmanos Cancer Institute in Detroit, US, were used. Each dataset includes a fused and pre-segmented USCT volume and the according cranio-caudal mammogram. Digital as well as analog mammograms were used. USCT volumes have a resolution of 0.5 mm/pixel at 450 × 450 pixel. The spacing between slices is 1 mm, the slice thickness is 4 mm. The number of slices varies depending on the size of the patient's breast. For evaluation purposes a criterion of inclusion is the visibility of a lesion in both images. The datasets were reviewed by an expert and the circumferences of the lesions were marked in both modalities.

The biomechanical models created for the evaluation consist of approximately 25,000 finite elements each. Different tissue types within the breast are not considered due to previous experiments[11] stating that there is no major effect in using a more complex model.

The accuracy of the registration can be estimated by the target registration error of a lesion visible in both modalities. Due to congruently overlaying images after carrying out the registration, the lesion marking can be compared directly and the distance of the centers as well as the overlap can be measured. The aim for clinical applicability is a large overlap of the contours and a small deviation between the center positions of the lesions to be clinically applicable.

Image registration was performed successfully in all 13 cases. Without any sagittal rotation of the datasets, a mean deviation of the centers of the marked lesions of 15.8 mm (median 13.2 mm, SD 11.4 mm) was achieved. The mean overlap of the lesion markings was 76% (median 85%, SD 32%).

To compensate for the rotation due to patient positioning and uncertain mammographic projection, datasets were rotated around the sagittal axis in the range of -30° to +30°. Using a manually determined rotation angle,

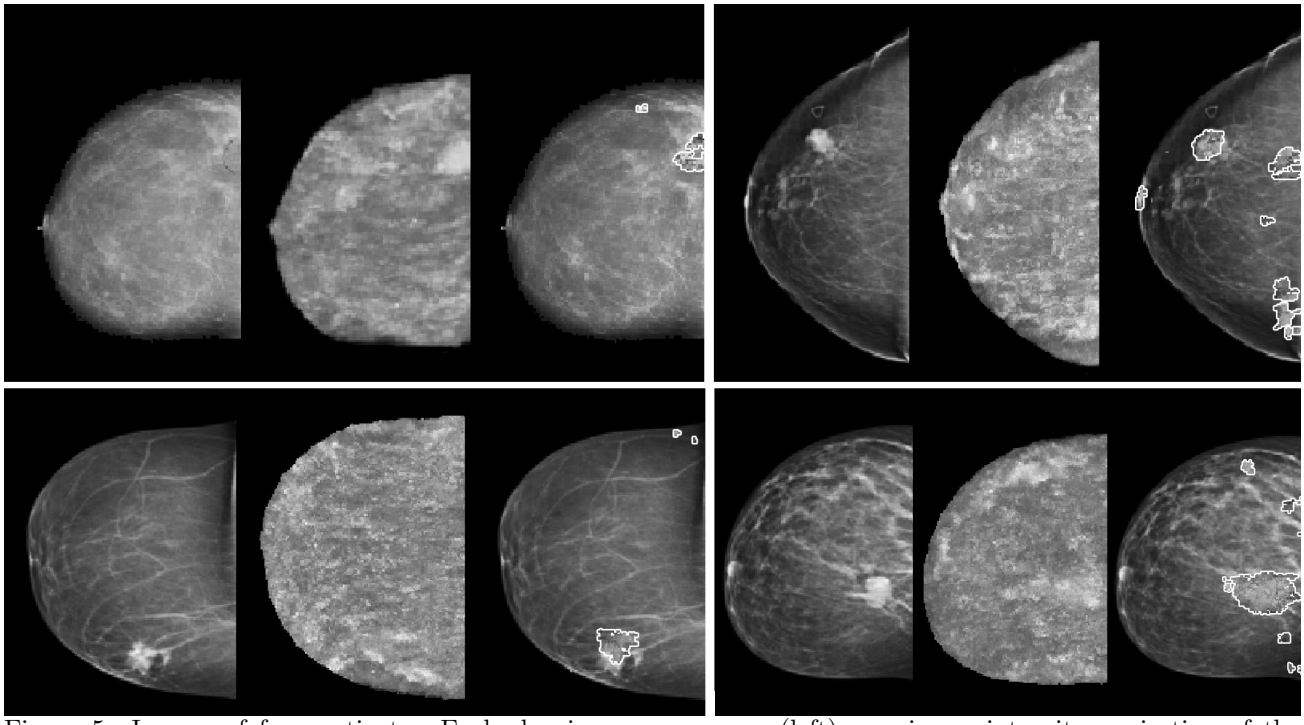

Figure 5: Images of four patients. Each showing mammogram (left), maximum intensity projection of the deformed USCT volume (middle) and fused image (right) highlighting suspect regions as colored overlay within the mammogram. Due to grayscale print, colored regions are outlined in this figure using a white contour.

the mean deviation of the marked lesion centers could be reduced to 7.6 mm (median 6.4 mm, SD 5.1 mm), the mean overlap was increased to 95% (median 100%, SD 96%).

However this correction had to be done manually for each dataset. Hence it avoids a completely automatic run and reproducible results. Therefore we applied the completely automatic rotation estimation based on image similarity between X-ray mammogram and projection image of the deformed USCT volume. Image similarity measures described in section 2.4 as well as registration accuracy were calculated for each rotation step. The registration accuracy at the rotation angle delivering the best image similarity value was taken as final result.

Gradient correlation was found to deliver the best results, i.e. the best registration accuracy. The mean deviation of the lesion centers was reduced to 10.4 mm (median 10.3 mm, SD 6.6 mm) using this measure. The mean overlap of lesion markings was increased to 93% (median 100%, SD 12%). Using correlation coefficient a mean deviation of 11.0 mm was obtained, normalized mutual information achieved a mean deviation of 11.3 mm.

All registration errors are below 20 mm. In 9 of 13 cases, a good registration accuracy below 15 mm was achieved. 11 of 13 cases showed an overlap of lesions above 90%.

Semitransparent overlay images for the mammograms were created for all 13 datasets. The thresholds a, b, c, and d were chosen patient-specifically by KCI. Resulting images are shown in Figure 5. The threshold overlays line up well with the lesions visible in the mammogram.

4. CONCLUSION

After promising results presented in Hopp et al.,[10,12] the now presented enhancement of our registration framework allows registration of a fused USCT volume with the corresponding mammogram in a completely automated workflow. The registration accuracy achieved affirms our former results. The average distance between the centers of lesions in the projected USCT volume and the X-ray mammogram is, for most cases, acceptable. The estimation of the rotation angle of the datasets is fully automated using image similarity measures. Hence no manual corrections have to be carried out to achieve a satisfying registration accuracy. Against the background

of uncertainties from marking the center and size of the lesion in both modalities, we believe these results are already adequate for further investigation of the correlation of mammograms with the new imaging modality USCT in future studies.

In addition we presented an overlay technique to visualize the information obtained from four modalities in one image. The colored overlays obtained from the USCT volume are rendered as semi-transparent overlay on the mammogram, enabling the radiologist to retrieve the morphology of the breast as well as quantitative tissue characterization at a glance. The threshold for speed of sound and attenuation were chosen patient-specifically. However an automatic thresholding is subject of current research. We expect this visualization of such quantitative measures to benefit multimodal breast cancer diagnosis, especially for patients with dense breasts.

To the author's knowledge the registration and image fusion of USCT volumes with X-ray mammograms has not been carried out before. The methodology allows combination of four modalities in one single image, which can be used for evaluation of the new imaging modality USCT as well as for combined breast cancer diagnosis. The information of USCT volumes has never been combined with X-ray mammography in such an intuitive way. The overlay technique allows a radiologist to explicitly highlight suspect regions of high speed of sound and attenuation within the mammogram. We expect this method to be beneficial for a more precise diagnosis. Moreover using USCT in addition to X-ray mammography may result in a cost reduction, and a faster and more comfortable examination, as USCT does not use contrast agent for a quantitative tissue characterization.

In future work we plan to expand the number of datasets to investigate our approach for clinical practice. Improvement of the overlay technique and interactive presentation within a diagnosis software might increase the usability for radiologists.

REFERENCES

[1] Fischer, T., Bick, U., and Thomas, A., "Mammographie-Screening in Deutschland," *Visions Journal* **15**, 62–67 (2007).

[2] American Cancer Society, "Breast cancer facts and figures 2011 - 2012." Atlanta: American Cancer Society, Inc. (2011).

[3] Sivaramakrishna, R. and Gordon, R., "Detection of breast cancer at a smaller size can reduce the likelihood of metastatic spread: A quantitative analysis"," *Academic Radiology* **4**(1), 8–12 (1997).

[4] DeMartini, W. and Lehman, C., "A review of current evidence-based clinical applications for breast magnetic resonance imaging.," *Top Magn Reson Imaging* **19**, 143–50– (June 2008).

[5] Kaiser, W. A., Fischer, H., Vagner, J., and Selig, M., "Robotic system for biopsy and therapy of breast lesions in a high-field whole-body magnetic resonance tomography unit," *Investigative Radiology* **35**(8), – (2000).

[6] Duric, N., Littrup, P., Poulo, L., Babkin, A., Pevzner, R., Holsapple, E., Rama, O., and Glide, C., "Detection of breast cancer with ultrasound tomography: First results with the computerized ultrasound risk evaluation (C.U.R.E)," *Medical Physics* **34**(2), 773–785 (2007).

[7] Duric, N., Littrup, P., Chandiwala-Mody, P., Li, C., Schmidt, S., Myc, L., Rama, O., Bey-Knight, L., Lupinacci, J., Ranger, B., Szczepanski, A., and West, E., "In-vivo imaging results with ultrasound tomography: Report on an ongoing study at the karmanos cancer institute," in [*Medical Imaging 2010: Ultrasonic Imaging, Tomography, and Therapy, Proceedings of the SPIE*], **7629**, 762905 (2010).

[8] Gemmeke, H. and Ruiter, N., "3d ultrasound computer tomography for medical imaging," *Nuclear Instruments and Methods in Physics Research Section A: Accelerators, Spectrometers, Detectors and Associated Equipment* **580**(2), 1057 – 1065 (2007).

[9] Greenleaf, J. F. and Bahn, R. C., "Clinical imaging with transmissive ultrasonic computerized tomography," *Journal of Computer Assisted Tomography* **5**(5), – (1981).

[10] Hopp, T., Holzapfel, M., Ruiter, N. V., Li, C., and Duric, N., "Registration of x-ray mammograms and three-dimensional speed of sound images of the female breast," in [*Medical Imaging 2010: Ultrasonic Imaging, Tomography, and Therapy, Proceedings of the SPIE*], D'hooge, J. and McAleavey, S. A., eds., *Medical Imaging 2010: Ultrasonic Imaging, Tomography, and Therapy* **7629**(1), 762905, SPIE (2010).

[11] Ruiter, N. V., Stotzka, R., Mueller, T. O., Gemmeke, H., Reichenbach, J. R., and Kaiser, W. A., "Model–based registration of x–ray mammograms and mr images of the female breast," *IEEE Transactions on Nuclear Science* **53**, 204 – 211 (2006).

[12] Hopp, T., Bonn, J., Ruiter, N. V., Sak, M., and Duric, N., "2d/3d image fusion of x-ray mammograms with speed of sound images: evaluation and visualization," in [*Medical Imaging 2010: Ultrasonic Imaging, Tomography, and Therapy, Proceedings of the SPIE*], **7968**(1), 79680L, SPIE (2011).

[13] Fang, Q. and Boas, D., "Tetrahedral mesh generation from volumetric binary and grayscale images," *IEEE International Symposium on Biomedical Imaging: From Nano to Macro, 2009. ISBI '09.* , 1142 –1145 (2009).

[14] Wellman, P. S., Howe, R. D., Dalton, E., and Kern, K. A., "Breast tissue stiffness in compression is correlated to histological diagnosis," technical report, Harvard BioRobotics Laboratory (1999).

[15] Hopp, T., Baltzer, P., Dietzel, M., Kaiser, W., and Ruiter, N., "2d/3d image fusion of x-ray mammograms with breast mri: visualizing dynamic contrast enhancement in mammograms," *International Journal of Computer Assisted Radiology and Surgery* **(in press)** (2011).

[16] Fitzpatrick, J. M. and Sonka, M., eds., [*Handbook of Medical Imaging – Volume 2. Medical Image Processing and Analysis*], vol. 2, SPIE Press Book (2000).

[17] Penney, G., Weese, J., Little, J., Desmedt, P., Hill, D., and Hawkes, D., "A comparison of similarity measures for use in 2d-3d medical image registration," *Medical Image Computing and Computer-Assisted Interventation - MICCAI'98* **1496**, 1153–1161 (1998).